

Detection of quantized mode families across multiple islands in intermediate-mass stars

SHRAVAN M. HANASOGE,¹ SHASHWAT CHAMOLI,¹ AND SUBRATA PANDA¹

¹*Tata Institute of Fundamental Research, Mumbai 400005, India*

ABSTRACT

Intermediate-mass δ Scuti stars occupy a transitional regime between low-mass stars, whose structure is relatively well understood, and high-mass stars, where the internal physics remains uncertain. Asteroseismology, which is a collection of techniques to infer the internal structure and rotation profiles of stars based on surface measurements of their oscillations, currently cannot be applied to most δ Scutis because of their complex and difficult-to-interpret oscillations. Here, we discover instances where *individual* oscillation spectra show multiple, discrete, and distinct large-frequency spacings. We propose that each sequence corresponds to a set of island modes whose eigenfunctions are concentrated around specific latitudes. For the spectra we show here, almost every consequential mode in the spectrum belongs to one sequence or another. The near-complete spectral quantization reveals a class of δ Scutis with highly ordered acoustic spectra, organized into multiple frequency combs. Our findings validate the acoustic ray-theoretic predictions of Lignières & Georgot (2008, 2009) and open the door to the systematic seismology of δ Scutis. The analysis also goes beyond using only large-amplitude sequences and indicates that low-amplitude modes distributed over the spectrum can provide crucial insight into stellar structure and dynamics.

1. INTRODUCTION

δ Scuti stars are rich laboratories for stellar astrophysics (Handler 2013), with their rapid rotation rates (Royer et al. 2007) playing a central role in shaping their structure and evolution. In some cases—such as Altair—the rotation approaches the Keplerian break-up velocity, leading to significant stellar deformation and marked oblateness (Bouchaud et al. 2020; Monnier et al. 2007). Structurally, δ Scutis possess a radiatively stable interior enveloped by a shallow convective layer near the surface (Handler et al. 2009), in contrast to solar-like stars, which feature an extensive outer convection zone surrounding a radiative core (Hekker & Christensen-Dalsgaard 2017).

Much of our current understanding of δ Scuti interiors arises from detailed modeling using 1D stellar evolution codes such as MESA (Paxton et al. 2010, 2013, 2015, 2018, 2019), and 2D non-perturbative simulations (Lignières et al. 2006; Reese et al. 2006; Lignières & Georgot 2008; Reese et al. 2008; Lignières & Georgot 2009; Reese et al. 2009, 2017; Reese 2022). However, direct inference of internal properties remains difficult due to the complexities involved in interpreting their oscillation spectra (Guzik 2021).

In solar-like stars, resonant oscillation modes are stochastically excited by supersonic near-surface turbulence, producing statistically well-characterized mode amplitudes for which a robust theoretical framework exists (Hekker & Christensen-Dalsgaard 2017). Their slow rotation maintains near-spherical symmetry, allowing modes to be identified and labeled using standard spherical-harmonic quantum numbers (Aerts et al. 2010; Aerts 2021). By contrast, rapid rotation in δ Scuti stars induces significant centrifugal distortion, invalidating spherical symmetry and requiring more appropriate basis functions, such as ellipsoidal harmonics, to describe the eigenfunctions (Dassios 2012). This spatial deformation, combined with the non-systematic excitation of modes by the opacity mechanism (Chevalier 1971), which assigns irregular amplitudes to modes, further complicates mode identification.

A final challenge arises from gravity darkening (Espinosa Lara & Rieutord 2011), an effect that modifies surface brightness due to rotationally induced oblateness. Since the degree of oblateness is typically unconstrained, this introduces additional uncertainty in mode visibility, further hindering robust mode identification in δ Scuti stars.

Numerical solvers developed to simulate wave propagation in rapidly rotating, deformed δ Scuti stars have provided valuable insights into their oscillation spectra (Lignières et al. 2006; Reese et al. 2006, 2008, 2009, 2017; Evano et al. 2019; Reese 2022). While these models do not explain the underlying wave-excitation mechanisms, they have enabled detailed characterization of mode families — specifically, whispering-gallery, island, and chaotic modes (Lignières & Geogteot 2008, 2009). The classical means by which to organize spectra is to identify unique large spacings, fold spectra at this frequency, and detect mode ladders. Slowly rotating stars fold at one, unique large spacing, the inverse diametric crossing time. However, the theoretical expectation for rapidly rotating stars (e.g., δ Scutis) is that they possess islands of oscillations, each of which corresponds to a regular sequence of modes organized around its specific $\Delta\nu$. Thus, an individual oscillation spectrum would show multiple large spacings, a significant departure from prior detections which have sought to identify a single large spacing for each star.

Ray theory, an asymptotic approximation valid in the high-frequency (short-wavelength) limit, serves as a useful framework for interpreting these modes (Lignières & Geogteot 2008, 2009; Pasek et al. 2011). In slowly rotating stars ($\Omega_\star/\Omega_K \ll 1$, where $\Omega_K = \sqrt{GM_\star/R_{\text{pole}}^3}$ is the Keplerian break-up velocity; Reese et al. 2006), the mode cavities are approximately spherical. In this regime, ray paths are stable, and oscillation modes can be labeled using spherical quantum numbers: harmonic degree ℓ , azimuthal order m , and radial order n . A single large frequency spacing ($\Delta\nu$) suffices to describe the separation between modes of consecutive radial order at fixed ℓ , particularly for low-degree modes ($\ell \leq 3$).

In contrast, rapidly rotating stars become significantly oblate, with equatorial radii exceeding polar radii ($R_{\text{eq}} > R_{\text{pole}}$). The resulting latitudinal dependence of mode cavities introduces geometric and dynamical complexity. Quantifying the transition between the slow- and fast-rotation regimes requires dedicated numerical modeling (Reese et al. 2006, 2008, 2009). As $\Omega_\star/\Omega_K \rightarrow 1$, the increasing oblateness leads to highly deformed mode cavities, the breakdown of global-mode quantization, and the emergence of chaotic and whispering-gallery modes (Lignières & Geogteot 2008, 2009; Pasek et al. 2011), complicating mode identification and limiting the effectiveness of asteroseismic analysis.

However, an intermediate regime exists in which δ Scuti stars rotate rapidly enough to exhibit deformation and in this process, create islands. In this regime, Lignières & Geogteot (2008, 2009) predict the appearance of quantized mode sequences termed 2-period and 6-period island modes, based on their surface geometries. The 2-period island modes complete a ray circuit in two bounces, traversing from pole to pole and exhibiting symmetry across the equator. These modes show minimal latitudinal variation, retain coherent surface patterns, and consequently exhibit strong photometric visibility—akin to $\ell = 0$ modes in non-rotating stars.

In contrast, 6-period island modes undergo six bounces per loop and display more intricate surface structures, leading to increased cancellation and reduced visibility. These are loosely analogous to $\ell > 0$ modes in slow rotators, though the analogy holds only in a limited sense. Both 2- and 6-period island modes are characterized by stable ray orbits and exhibit well-defined large frequency spacings (Lignières & Geogteot 2008, 2009; Pasek et al. 2011), making them promising candidates for mode identification and asteroseismic diagnostics in moderately rotating δ Scuti stars.

Due to stellar oblateness, higher latitudes lie closer to the stellar center and are generally hotter, as described by von Zeipel’s theorem (Zeipel 1924). As a result, ray paths associated with the 2-period island modes are both geometrically shorter and traverse regions of higher sound speed compared to those of the 6-period family. Consequently, the travel times for 2-period rays are shorter, leading to larger frequency spacings ($\Delta\nu$) relative to the 6-period modes. Furthermore, the 2-period ray paths penetrate deeper into the stellar interior, making their corresponding $\Delta\nu$ values more sensitive to the mean stellar density (Reese et al. 2008; Mirouh et al. 2018).

In the ray-theoretic framework, only discrete values of $\Delta\nu$ yield closed-loop resonances. At moderate rotation rates ($0.3 \lesssim \Omega_\star/\Omega_K \lesssim 0.6$), this quantization condition implies that only a finite number of regular mode sequences — i.e., distinct island families — exist. As the rotation rate increases, these islands progressively shrink, and the ray dynamics eventually enter a chaotic regime beyond a critical threshold, leading to a breakdown of the quantization principle for some of the islands. In a stable regime, two rays that start in close proximity at the surface remain so throughout their propagation lifetimes. In a chaotic regime, the ray path is sensitively dependent on the initial condition, and two initially proximal rays can end up taking very different paths. Regular sequences can thus be harder to identify or may not exist prominently in this latter parameter range. Conversely, at very low rotation rates, all island families converge to a single large spacing, characteristic of spherical stars.

Observational studies have predominantly focused on regular oscillation patterns in slowly rotating stars, where a unique large frequency spacing ($\Delta\nu$) characterizes the mode structure. However, as noted by García Hernández et al. (2015a,b); Páparó et al. (2016a,b); Bedding et al. (2020), the oscillation spectra of some near-Zero Age Main Sequence

(ZAMS) δ Scuti stars exhibit regular sequences, each associated with a distinct value of $\Delta\nu$. We argue that these prior observations — as well as our present detections of multiple large spacings — are in agreement with the ray-theory predictions developed by [Lignières & Georgeot \(2008, 2009\)](#) and [Pasek et al. \(2011\)](#). Specifically, the presence of multiple discrete $\Delta\nu$ values corresponds to quantized island modes in moderately rotating, oblate stellar models.

2. DATA

We investigate oscillation properties in a sample of 5,381 δ Scuti stars from the TESS catalog ([Singh et al. 2025](#)). Among these, regular frequency spacings were detected in 300 stars, consistent with the occurrence rate reported by [Bedding et al. \(2020\)](#). The corresponding large frequency separations ($\Delta\nu$) for these stars were documented by [Singh et al. \(2025\)](#). In the present study, we set aside these stars and focus on the remainder of the sample to identify frequency patterns that may be too subtle or irregular to be detected by automated algorithms. We followed the approach outlined by [Bedding et al. \(2020\)](#), i.e., visually adjusted the $\Delta\nu$ values until ridge-like features appear in the échelle diagrams. The visualization was performed carefully to ensure that peaks that have extremely faint amplitudes but form regular patterns are retained. Particularly challenging is the significant variability in amplitude that a single ridge can have - it is difficult to locate the small-amplitude peaks. Consequently, this method is time-consuming and requires patience in examining each spectrum. There are likely far more accurate and faster automated ways to achieve this search, but we have been unable to construct a suitably successful algorithm.

Figure 1 presents the échelle diagrams corresponding to the oscillation spectrum of TIC 33248782. In each panel, we identify multiple values of the large frequency separation ($\Delta\nu$) at which the modes exhibit regular alignment, with the spacings varying by approximately 30–40% for this star. Among the three panels, the diagram with $\Delta\nu = 5.86, \text{d}^{-1}$ is a plausible candidate for the “correct” spacing, as it reveals three faint, ridge-like features that may correspond to the $\ell = 0, 1,$ and 2 modes—or possibly to rotationally split components. Nevertheless, the remaining two diagrams also display distinct elongated features, suggesting the presence of additional independent mode sequences with different regular spacings. Similar analyses for TIC 89547212, TIC 174206494, TIC 233162061, and TIC 248400677 are shown in Figures 2–5, respectively. Each star exhibits multiple faint, regularly spaced mode sequences at distinct values of $\Delta\nu$, reinforcing the hypothesis that such multi-sequence patterns are a common feature in moderately rotating δ Scuti stars.

Numerous modes in Figure 1 appear to belong to three distinct sequences. On the one hand, this may be due to mislabelling; for example, the green diamond and red asterisk in the $5.86, \text{d}^{-1}$ échelle diagram have been identified as independent sequences, although they may trace the same underlying feature. The resonant frequency of the i th mode (where i is an integer representing the mode’s quantum number) of the k th sequence can be expressed as $\nu^{(k)}_i = \Delta\nu_k i + \alpha_k$, where α_k is a sequence-specific offset. Here, we focus on the inter-mode spacings at different ‘radial orders’ and not on the perturbative multiplet splittings that rotation induces ([Ledoux 1949](#)). Rotation non-perturbatively affects mode eigenfunctions when $\Omega/\Omega_K \gtrsim 0.3$ ([Reese et al. 2006](#)), the relevant regime for these stars, confining them to specific latitudes and altering the entire structure of the associated resonant cavities. For a mode that appears in both sequences k and k' , the frequencies must satisfy $i\Delta\nu_k + \alpha_k = i'\Delta\nu_{k'} + \alpha_{k'}$ and $(i+p)\Delta\nu_k + \alpha_k = (i'+q)\Delta\nu_{k'} + \alpha_{k'}$, where p, q are small integers representing the average spacing between overlapping modes. Subtracting these two equations yields a simple relation for the ratio of large separations: $\Delta\nu_{k'}/\Delta\nu_k = p/q$.

In Figure 1, the pairwise ratios of large spacings are $8.8/5.6 = 1.57 \approx 3/2$, $9.706/5.86 = 1.66 \approx 5/3$, and $9.706/8.8 = 1.10$. Two of these ratios are well approximated by small-integer fractions. This applies to the spacings identified in the other figures as well, although not all ratios can be represented as fractions of small integers. Modes shared between different ladders satisfy the quantization criteria of multiple sequences and may be interpreted as analogues of mixed modes. Alternatively, they could represent nearly degenerate mode pairs, where one mode has an amplitude too low to be detected. The commensurability of the acoustic spacings suggests that the star supports multiple interacting quantization schemes, consistent with the behavior of island modes in moderately rotating δ Scuti stars. Comparing the $5.86, \text{d}^{-1}$ and $8.8, \text{d}^{-1}$ échelle diagrams in Figure 1, we observe that every third mode marked by red asterisks aligns with every second mode marked by pink hashes. A similar overlap is seen between every third black square and every second red cross. Additionally, every fifth blue circle, black square, and red asterisk coincide with every third brown dashed-circle, green semicircle, and brown dashed-circle, respectively.

[Paparó et al. 2016a,b](#) identified oscillation spectra exhibiting multiple regular sequences ν_i at distinct values of $\Delta\nu$, which they interpreted as linear combinations $\nu_i = k\Delta\nu/2 + k'\Omega_*$, where k, k' are integers, and the star was assumed to have only one large spacing. The perturbative treatment of rotation as a splitting breaks down when

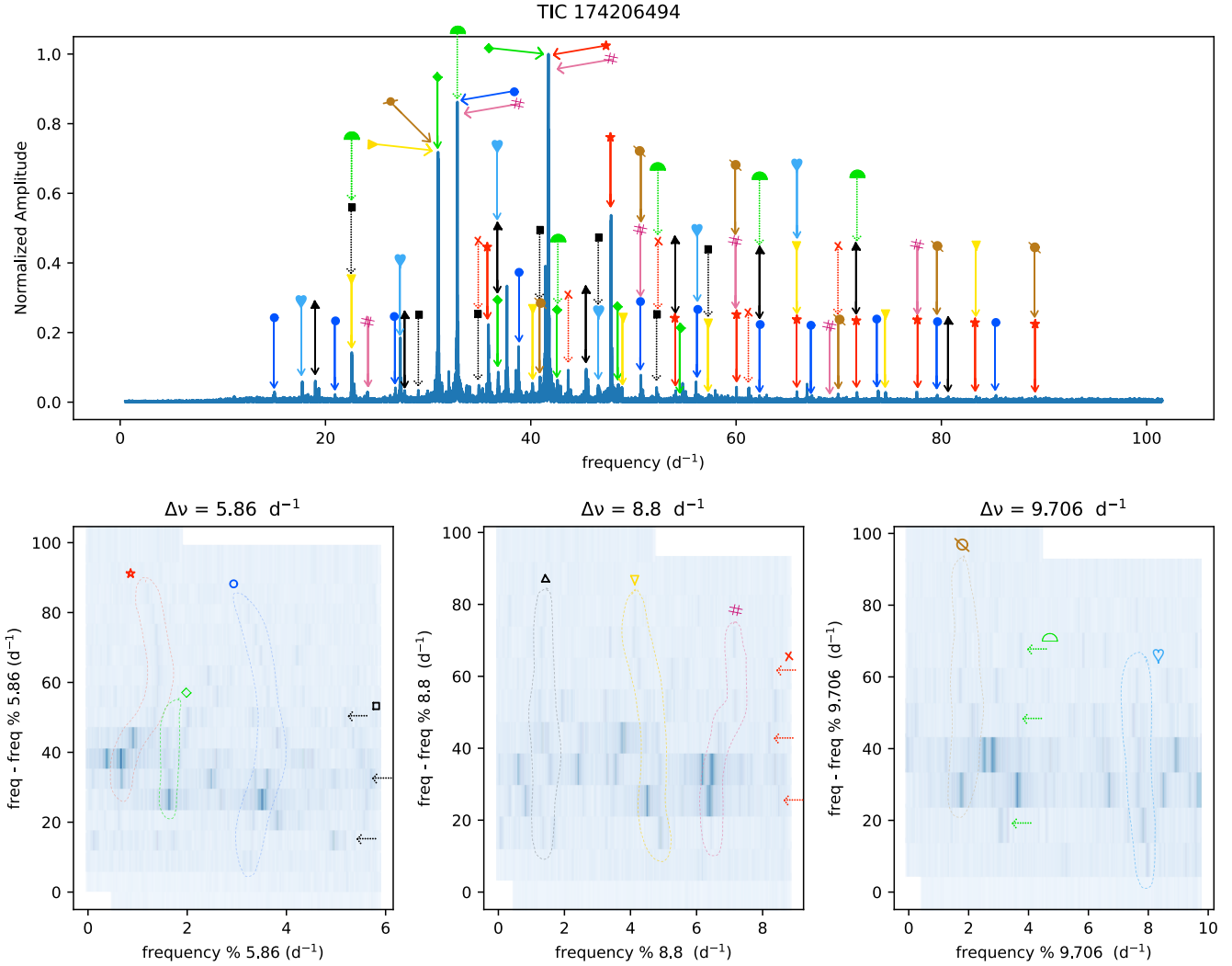


Figure 1. Normalized power spectrum and échelles at three values of large spacings for a δ Scuti. Each sequence in the échelle diagrams is marked using faint dashed lines or arrows of different colours and a symbol on top. The markings are intentionally kept subtle to avoid distracting from the features themselves. The same color and symbol are used to identify the corresponding modes in the power spectrum above. Some modes appear to be associated with two different sequences (indicated by dual arrows), although nearby unmarked peaks may help resolve this apparent degeneracy. Notably, nearly all significant peaks in the power spectrum are associated with one of the identified sequences, approaching a state of near-complete spectral quantization.

145 $\Omega_*/\Omega_K \gtrsim 0.3$ (Reese et al. 2006), and the regularity of inter-mode spacings across numerous radial orders challenges
 146 this interpretation. Bedding et al. (2020) also inferred multiple large spacings but simply averaged over the different
 147 values they obtained. However, our findings reveal variations in $\Delta\nu$ of up to 30–40%, which is problematic for the
 148 averaging approach. Similarly Ramón-Ballesta et al. 2021 reported the occurrences of multiple frequency regularities
 149 in the spectra of δ Scuti stars. Lastly, such large differences in $\Delta\nu$ indicate that more nuance is required to relate it
 150 to the mean stellar density. For comparison, $\Delta\nu$ exhibits variation at the level of only 1–3% (Huber et al. 2011) in
 151 main-sequence solar-like oscillators.

152 A likely interpretation of these observations is that rapid stellar rotation induces significant distortion, leading to the
 153 formation of latitudinally confined oscillation modes, known as *island modes* (Reese et al. 2009). The geometric path
 154 lengths of these modes govern their associated large frequency spacings ($\Delta\nu$). Consequently, the presence of multiple
 155 regular mode sequences can be understood as the manifestation of island modes concentrated at different latitudinal
 156 bands. As discussed earlier, island modes near the equator (e.g., 6-period modes) follow longer and slower ray paths,

resulting in greater travel times and appearing as regular sequences at lower values of $\Delta\nu$. In contrast, island modes confined to higher latitudes (e.g., 2-period modes) traverse shorter, faster paths and thus have shorter travel times, manifesting at relatively higher $\Delta\nu$.

We perform a back-of-the-envelope calculation to model these effects. This analysis is designed to build physical intuition for individual stars with multiple large spacings and the inferences may therefore be erroneous. It also reveals how the hierarchy of inter-mode spacings encodes geometrical and structural information. Since stellar geometry is strongly influenced by rotation, these parameters may be used to directly constrain the rotation rate. These relations are not intended to accurately capture the effect of rotation. The stellar oblateness is defined as $\varepsilon = \frac{R_{\text{eq}} - R_{\text{pole}}}{R_{\text{eq}}} \approx \alpha^2 \left(\frac{\Omega_\star}{\Omega_K} \right)^2$, where R_{eq} and R_{pole} denote the equatorial and polar radii, respectively (Goupil et al. 2000). Pérez Hernández et al. (1999) and Paxton et al. (2019) estimated the coefficient $\alpha^2 \approx 0.5$ but we leave it here in symbolic form. The radius at a given colatitude θ for an ellipsoid is approximately given by $R(\theta) \approx R_{\text{pole}} (1 + \varepsilon \cos^2 \theta)$; other models of oblateness include predictions from Roche models (Pérez Hernández et al. 1999) and perturbative treatments of centrifugal distortion (Saio 1981). All island modes considered here propagate to the surface and reflect at their upper turning points. Since the sound speed is lowest in the outer layers, waves spend the longest time in these regions. Thus, we crudely approximate the travel time of an island-mode family as being proportional to the stellar radius at the corresponding latitude, although this may break down at higher rotation rates. This implies a latitudinal dependence of the large frequency spacing, such that $\Delta\nu \propto R^{-1}(\theta) \approx (1 + \varepsilon \cos^2 \theta)^{-1}$.

Denote the set of N observed large frequency spacings by $\Delta\nu_0 > \Delta\nu_1 > \dots > \Delta\nu_N$, where $\Delta\nu_0$ corresponds to modes concentrated near the poles — i.e., those closest to the rotation axis and therefore least influenced by centrifugal distortion. In general, we observe at most three distinct values of $\Delta\nu$ per spectrum, i.e., $N_{\text{max}} \sim 3$.

The ratios of these large spacings can, in principle, be used to estimate the effective oblateness of the star via the relation

$$\varepsilon \cos^2 \theta_i = \beta^2 \left(\frac{\Delta\nu_0}{\Delta\nu_i} - 1 \right), \quad (1)$$

where β^2 is a proportionality constant that depends on the geometry of the resonance cavity, i.e., the number of bounces and the exact ray path, details of the structure of the star, etc. The 6-period island mode for instance bounces 6 times to complete a circuit, whereas the 2-period mode (2 bounces). That the ratio of the large spacings is generally on the order of 30-40% despite the significant differences between the mode paths of the two families suggests that the oblateness cannot be particularly large, although detailed calculations are required to establish these values.

For the star shown in Figure 1, we identify three distinct values of $\Delta\nu$. Assuming that the largest value, $\Delta\nu_0$, corresponds to near-polar modes, we apply equation 1 to estimate the effective oblateness. The smallest observed large spacing, $\Delta\nu_N$, is attributed to equatorially confined modes, which have the longest path lengths (correspondingly, travel times) and therefore the lowest frequencies. This enables us to place a lower bound on the oblateness:

$$\varepsilon = \frac{\beta^2}{\cos^2 \theta_N} \left(\frac{\Delta\nu_0}{\Delta\nu_N} - 1 \right) \geq \beta^2 \left(\frac{\Delta\nu_0}{\Delta\nu_N} - 1 \right). \quad (2)$$

Using equation 2, we can then place a corresponding lower bound on the rotation rate:

$$\varepsilon \approx \alpha^2 \left(\frac{\Omega_\star}{\Omega_K} \right)^2 \Rightarrow \Omega_\star \approx \Omega_K \sqrt{\varepsilon} \geq \frac{\beta \Omega_K}{\alpha} \sqrt{\frac{\Delta\nu_0}{\Delta\nu_N} - 1}. \quad (3)$$

3. DISCUSSION

Two features worth emphasizing are the remarkable agreement with ray-theoretic predictions (Lignières & Geogteot 2008, 2009; Pasek et al. 2011), and the unexpectedly strong manifestation of spectral quantization. The resonant frequencies are organized in accordance with the asymptotic relation (equation 30 of Lignières & Geogteot 2009), given by $\nu = n' \Delta_n + \ell' \Delta'_\ell + \alpha$, where n' and ℓ' are the modified radial order and harmonic degree, respectively—quantum numbers associated with oscillations in an oblate geometry—and Δ' denotes the large spacing specific to each island-mode family. This interpretation also implies that caution is warranted when using the large frequency spacing $\Delta\nu$ as a direct proxy for mean stellar density. Only those island modes that penetrate deep into the stellar interior provide meaningful constraints on the core density. Thus, accurate mode identification becomes essential. However, in slowly rotating stars, this correlation may still be valid, as the variation in $\Delta\nu$ across mode families is likely

Stellar ID	ϵ	Ω_*/Ω_K	M_* (M_\odot)	R_* (R_\odot)	$\Omega_K/(2\pi)$ (d^{-1})	$\Omega_{\text{seismic}}/(2\pi)$ (d^{-1})	$v \sin i$ (km s^{-1})	$\Omega_{\text{spectro}}/(2\pi)$ (d^{-1})
TIC33248782	≥ 0.14	≥ 0.54	1.797	1.8814	4.49	reference	228.636	≥ 2.40
TIC89547212	≥ 0.06	≥ 0.34	1.919	1.8038	4.93	≥ 1.66	--	--
TIC174206494	≥ 0.13	≥ 0.5	1.809	1.6926	5.27	≥ 2.64	--	--
TIC233162061	≥ 0.1	≥ 0.45	1.912	1.5872	5.97	≥ 2.65	200.772	≥ 2.50
TIC248400677	≥ 0.1	≥ 0.437	--	--	--	--	--	--

Table 1. Columns from left to right denote the (1) TIC IDs of the stars analyzed, (2) deformation calculated using equation 2, (3) rotation rates expressed in terms of the critical rotation frequency, (4) masses and (5) radii taken from Gaia DR3 (Sartoretti et al. 2023), (6) critical rotation $\Omega_K = \sqrt{GM_*/R_*^3}$, (7) asteroseismically calculated rotation using columns 3 and 6, (8) Gaia DR3-provided spectroscopically measured line-of-sight projected velocity, and (9) the rotation rate obtained from the spectroscopic rotational velocity through the relation $v \sin i/(2\pi R_*) \leq v/(2\pi R_*) = \Omega_{\text{spectro}}/(2\pi)$. We use the spectroscopic rotation measurement for TIC33248782 to estimate β/α , which is why we do not specify Ω_{seismic} for this star. We apply the value of β/α to estimate the oblateness and rotation rates for the other stars in this sample. TIC233162061 provides an opportunity to (successfully) validate this approach, although the close agreement between the inferred and spectroscopic bounds may well be a coincidence. The analytical framework here is designed to refine our physical intuition, and not meant as a replacement for sophisticated computational models; the inferences are consequently possibly erroneous.

minimal. We apply the asymptotic framework outlined in equations (1–3) to estimate lower bounds on oblateness and rotation rate, as summarized in Table 1. Here, we use the spectroscopically-inferred lower bound for the rotation rate for TIC33248782 to estimate β/α from equation (3). Several assumptions go into drawing this inference - (1) that the spacings obtained from the spectrum actually capture the full dynamic range of $\Delta\nu$, i.e., both the polar and equatorial diametric crossings, (2) the asymptotic formulae for oblateness, latitude-dependent radius, and the travel-time approximation are accurate, (3) the value β/α remains constant over this range of Ω_*/Ω_K considered here. Assumption (1) is satisfied if our mode identifications are precise; however, concluding this requires the application of a sophisticated numerical or computational model. Thus, these inferences must be treated with appropriate caution and at best represent a starting point for a more thorough investigation.

Equations (1)–(3) likely overestimate both the oblateness and the rotation rate, as the assumed correspondence between travel time and stellar radius is approximate and may introduce systematic errors. A more robust approach involves the use of stellar models tailored to rapidly rotating δ Scuti stars, such as those computed with the numerical frameworks developed by Lignières et al. (2006) and Reese et al. (2006), which account for centrifugal distortion and its influence on oscillation modes. By matching the multiple observed large frequency spacings to those predicted by such simulations, it may be possible to constrain the stellar structure and rotation rate with significantly greater precision. The organization of the oscillations into regular sequences provides a powerful means by which to classify spectra and compare observations with numerical predictions.

In helioseismology and the asteroseismology of slowly rotating stars, inversion techniques rely on sets of modes with different sensitivity kernels to image distinct regions of the solar or stellar interior. The spatial resolution of the resulting image improves with the number of observed modes, as the seismic point-spread function becomes more localized. Crucially, however, all such modes belong to a single large-spacing family. For rapidly rotating stars, the analog to this scenario is the presence of multiple regular mode sequences, each associated with a distinct large spacing. Each sequence probes a different region of the star, determined by the latitudinal confinement of its associated island-mode family. Therefore, combining multiple mode sequences can provide complementary information about the stellar interior. The more large spacings that are observed, the better the overall model constraints—since each spacing corresponds to a distinct, stable resonant cavity within the oblate stellar geometry. The measurements presented here thus offer the potential to significantly advance our understanding of δ Scuti oscillations and, more broadly, to improve inferences of their internal structure and dynamics.

SMH, SP and SC acknowledge support from the Department of Atomic Energy, Government of India, under Project Identification No. RTI 4002. This research was supported in part by a generous donation (from the Murty Trust) aimed at enabling advances in astrophysics through the use of machine learning. Murty Trust, an initiative of the Murty Foundation, is a not-for-profit organisation dedicated to the preservation and celebration of culture, science, and knowledge systems born out of India. The Murty Trust is headed by Mrs. Sudha Murty and Mr. Rohan Murty.

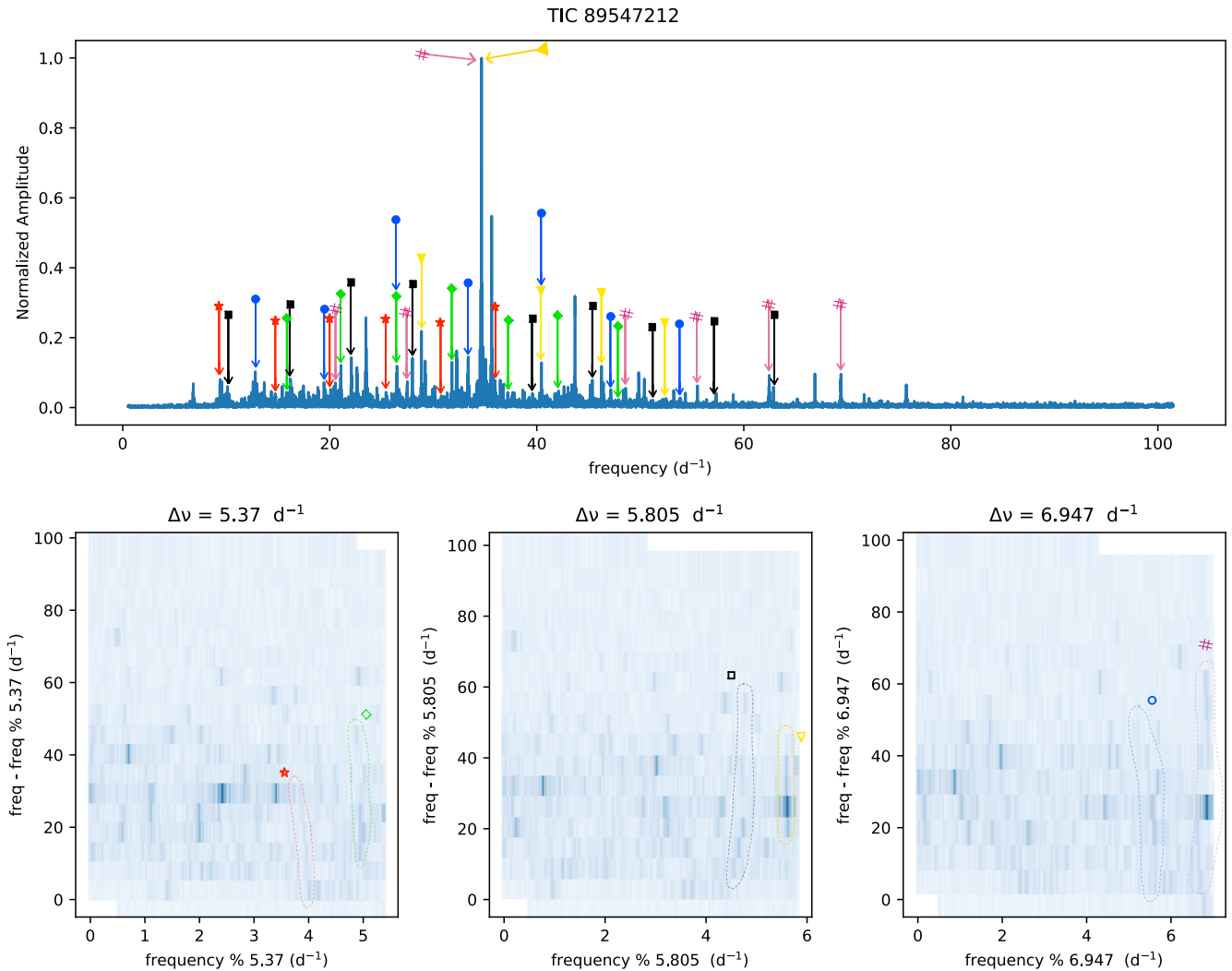


Figure 2. Normalized power spectrum and échelles at three values of large spacings for a δ Scuti. Each sequence in the échelle diagrams is marked using faint dashed lines of different colours and a symbol on top. The markings are intentionally kept subtle to avoid distracting from the features themselves. The same color and symbol are used to identify the corresponding modes in the power spectrum above. Some modes appear to be associated with two different sequences (indicated by dual arrows), although nearby unmarked peaks may help resolve this apparent degeneracy. Notably, nearly all significant peaks in the power spectrum are associated with one of the identified sequences, approaching a state of near-complete spectral quantization.

REFERENCES

- 235 Aerts, C. 2021, *Rev. Mod. Phys.*, 93, 015001,
 236 doi: [10.1103/RevModPhys.93.015001](https://doi.org/10.1103/RevModPhys.93.015001)
- 237 Aerts, C., Christensen-Dalsgaard, J., & Kurtz, D. W. 2010,
 238 *Asteroseismology* (Springer Dordrecht),
 239 doi: [10.1007/978-1-4020-5803-5](https://doi.org/10.1007/978-1-4020-5803-5)
- 240 Bedding, T. R., Murphy, S. J., Hey, D. R., et al. 2020,
 241 *Nature*, 581, 147–151, doi: [10.1038/s41586-020-2226-8](https://doi.org/10.1038/s41586-020-2226-8)
- 242 Bouchaud, K., Domiciano de Souza, A., Rieutord, M.,
 243 Reese, D. R., & Kervella, P. 2020, *A&A*, 633, A78,
 244 doi: [10.1051/0004-6361/201936830](https://doi.org/10.1051/0004-6361/201936830)
- 245 Chevalier, C. 1971, *A&A*, 14, 24
- 246 Dassios, G. 2012, *Ellipsoidal Harmonics: Theory and*
 247 *Applications*, *Encyclopedia of Mathematics and its*
 248 *Applications* (Cambridge University Press)
- 249 Espinosa Lara, F., & Rieutord, M. 2011, *A&A*, 533, A43,
 250 doi: [10.1051/0004-6361/201117252](https://doi.org/10.1051/0004-6361/201117252)

TIC 33248782

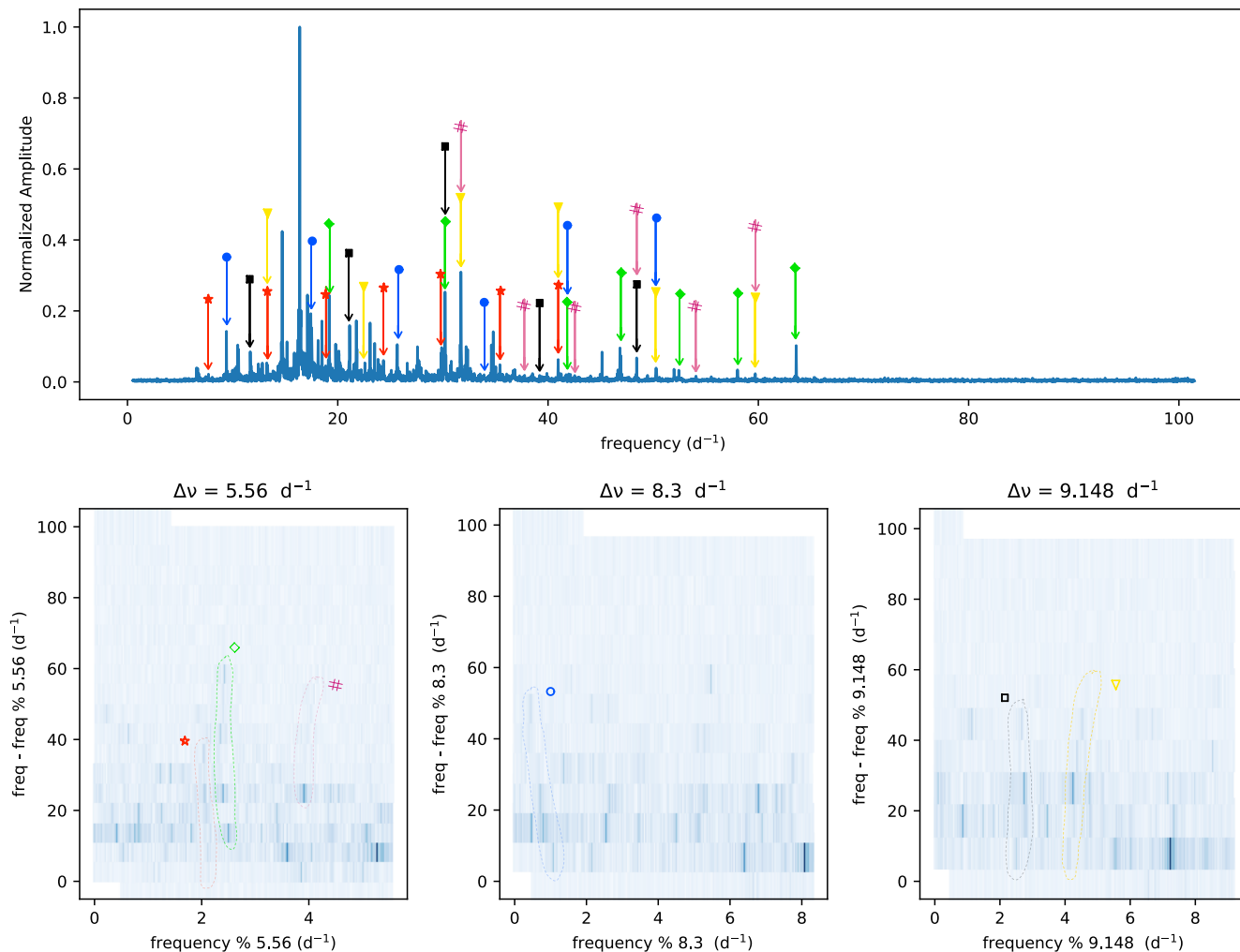


Figure 3. Normalized power spectrum and échelles at three values of large spacings for a δ Scuti. Each sequence in the échelle diagrams is marked using faint dashed lines of different colours and a symbol on top. The markings are intentionally kept subtle to avoid distracting from the features themselves. The same color and symbol are used to identify the corresponding modes in the power spectrum above. Some modes appear to be associated with two different sequences (indicated by dual arrows), although nearby unmarked peaks may help resolve this apparent degeneracy. Notably, nearly all significant peaks in the power spectrum are associated with one of the identified sequences, approaching a state of near-complete spectral quantization.

- 251 Evano, B., Lignières, F., & Georgeot, B. 2019, *A&A*, 631,
 252 A140, doi: [10.1051/0004-6361/201936459](https://doi.org/10.1051/0004-6361/201936459)
- 253 García Hernández, A., Lignières, F., Balona, L., et al.
 254 2015a, in *European Physical Journal Web of Conferences*,
 255 Vol. 101, *European Physical Journal Web of Conferences*,
 256 06026, doi: [10.1051/epjconf/201510106026](https://doi.org/10.1051/epjconf/201510106026)
- 257 García Hernández, A., Martín-Ruiz, S., Monteiro, M. J. P.
 258 F. G., et al. 2015b, *The Astrophysical Journal Letters*,
 259 811, L29, doi: [10.1088/2041-8205/811/2/L29](https://doi.org/10.1088/2041-8205/811/2/L29)
- 260 Goupil, M. J., Dziembowski, W. A., Pamyatnykh, A. A., &
 261 Talon, S. 2000, in *Astronomical Society of the Pacific*
 262 *Conference Series*, Vol. 210, *Delta Scuti and Related*
 263 *Stars*, ed. M. Breger & M. Montgomery, 267
- 264 Guzik, J. A. 2021, *Frontiers in Astronomy and Space*
 265 *Sciences*, 8, doi: [10.3389/fspas.2021.653558](https://doi.org/10.3389/fspas.2021.653558)
- 266 Handler, G. 2013, *Asteroseismology* (Springer Netherlands),
 267 207–241, doi: [10.1007/978-94-007-5615-1_4](https://doi.org/10.1007/978-94-007-5615-1_4)
- 268 Handler, G., Guzik, J. A., & Bradley, P. A. 2009, in *AIP*
 269 *Conference Proceedings* (AIP), 403–409,
 270 doi: [10.1063/1.3246528](https://doi.org/10.1063/1.3246528)
- 271 Hekker, S., & Christensen-Dalsgaard, J. 2017, *The*
 272 *Astronomy and Astrophysics Review*, 25,
 273 doi: [10.1007/s00159-017-0101-x](https://doi.org/10.1007/s00159-017-0101-x)
- 274 Huber, D., Bedding, T. R., Stello, D., et al. 2011, *The*
 275 *Astrophysical Journal*, 743, 143,
 276 doi: [10.1088/0004-637X/743/2/143](https://doi.org/10.1088/0004-637X/743/2/143)

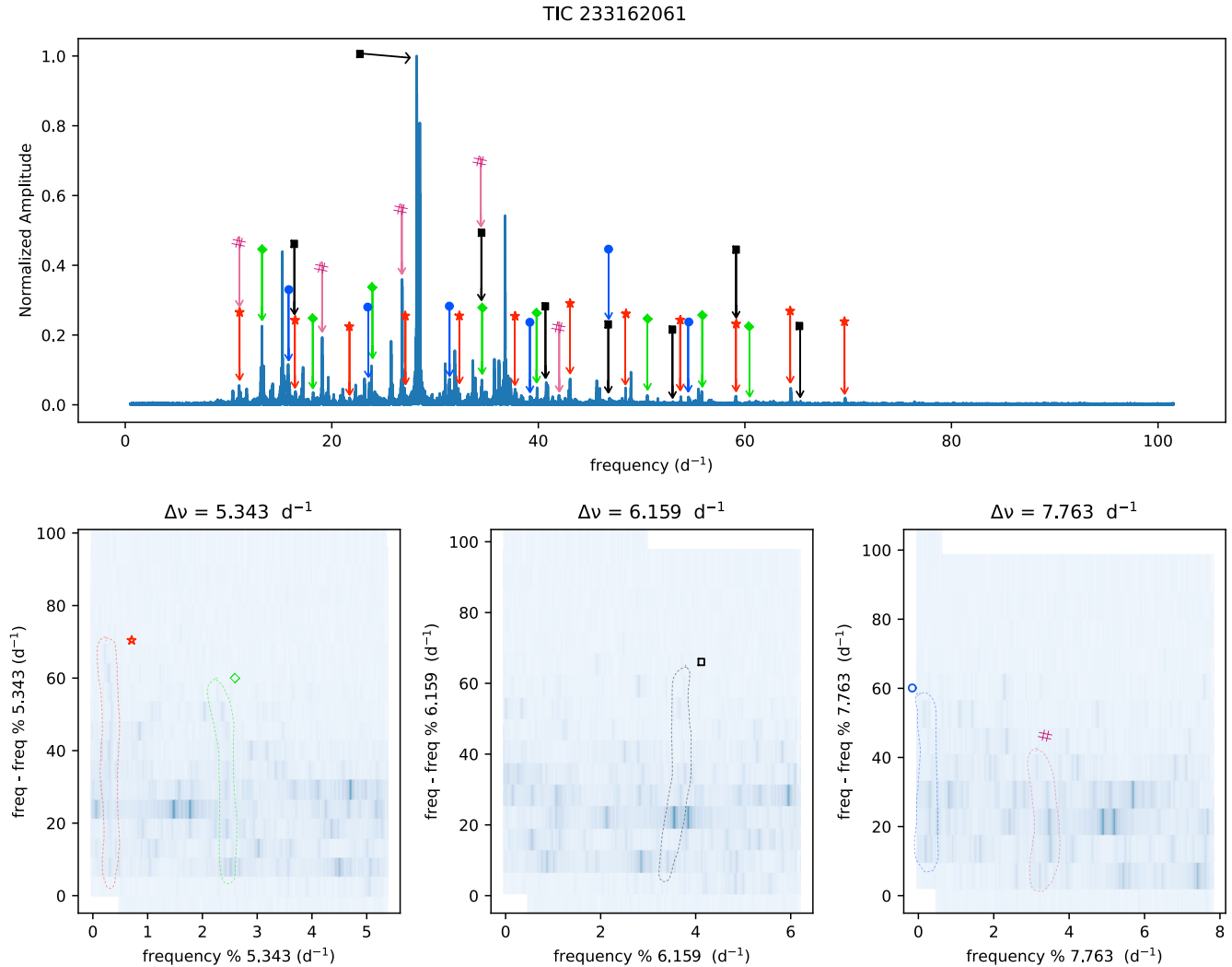


Figure 4. Normalized power spectrum and échelles at three values of large spacings for a δ Scuti. Each sequence in the échelle diagrams is marked using faint dashed lines of different colours and a symbol on top. The markings are intentionally kept subtle to avoid distracting from the features themselves. The same color and symbol are used to identify the corresponding modes in the power spectrum above. Some modes appear to be associated with two different sequences (indicated by dual arrows), although nearby unmarked peaks may help resolve this apparent degeneracy. Notably, nearly all significant peaks in the power spectrum are associated with one of the identified sequences, approaching a state of near-complete spectral quantization.

- 277 Ledoux, P. 1949, *Memoires of the Societe Royale des*
 278 *Sciences de Liege*, 9, 3
- 279 Lignières, F., & Geogot, B. 2008, *Physical Review E*, 78,
 280 doi: [10.1103/physreve.78.016215](https://doi.org/10.1103/physreve.78.016215)
- 281 —. 2009, *A&A*, 500, 1173,
 282 doi: [10.1051/0004-6361/200811165](https://doi.org/10.1051/0004-6361/200811165)
- 283 Lignières, F., Rieutord, M., & Reese, D. 2006, *Astronomy*
 284 *& Astrophysics*, 455, 607–620,
 285 doi: [10.1051/0004-6361:20065015](https://doi.org/10.1051/0004-6361:20065015)
- 286 Mirouh, G. M., Angelou, G. C., Reese, D. R., & Costa, G.
 287 2018, *Monthly Notices of the Royal Astronomical*
 288 *Society: Letters*, 483, L28, doi: [10.1093/mnrasl/sly212](https://doi.org/10.1093/mnrasl/sly212)
- 289 Monnier, J. D., Zhao, M., Pedretti, E., et al. 2007, *Science*,
 290 317, 342–345, doi: [10.1126/science.1143205](https://doi.org/10.1126/science.1143205)
- 291 Papparo, M., Benkő, J. M., Hareter, M., & Guzik, J. A.
 292 2016a, *The Astrophysical Journal*, 822, 100,
 293 doi: [10.3847/0004-637X/822/2/100](https://doi.org/10.3847/0004-637X/822/2/100)
- 294 —. 2016b, *The Astrophysical Journal Supplement Series*,
 295 224, 41, doi: [10.3847/0067-0049/224/2/41](https://doi.org/10.3847/0067-0049/224/2/41)
- 296 Pasek, M., Geogot, B., Lignières, F., & Reese, D. R. 2011,
 297 *Physical Review Letters*, 107,
 298 doi: [10.1103/physrevlett.107.121101](https://doi.org/10.1103/physrevlett.107.121101)
- 299 Paxton, B., Bildsten, L., Dotter, A., et al. 2010, *The*
 300 *Astrophysical Journal Supplement Series*, 192, 3,
 301 doi: [10.1088/0067-0049/192/1/3](https://doi.org/10.1088/0067-0049/192/1/3)

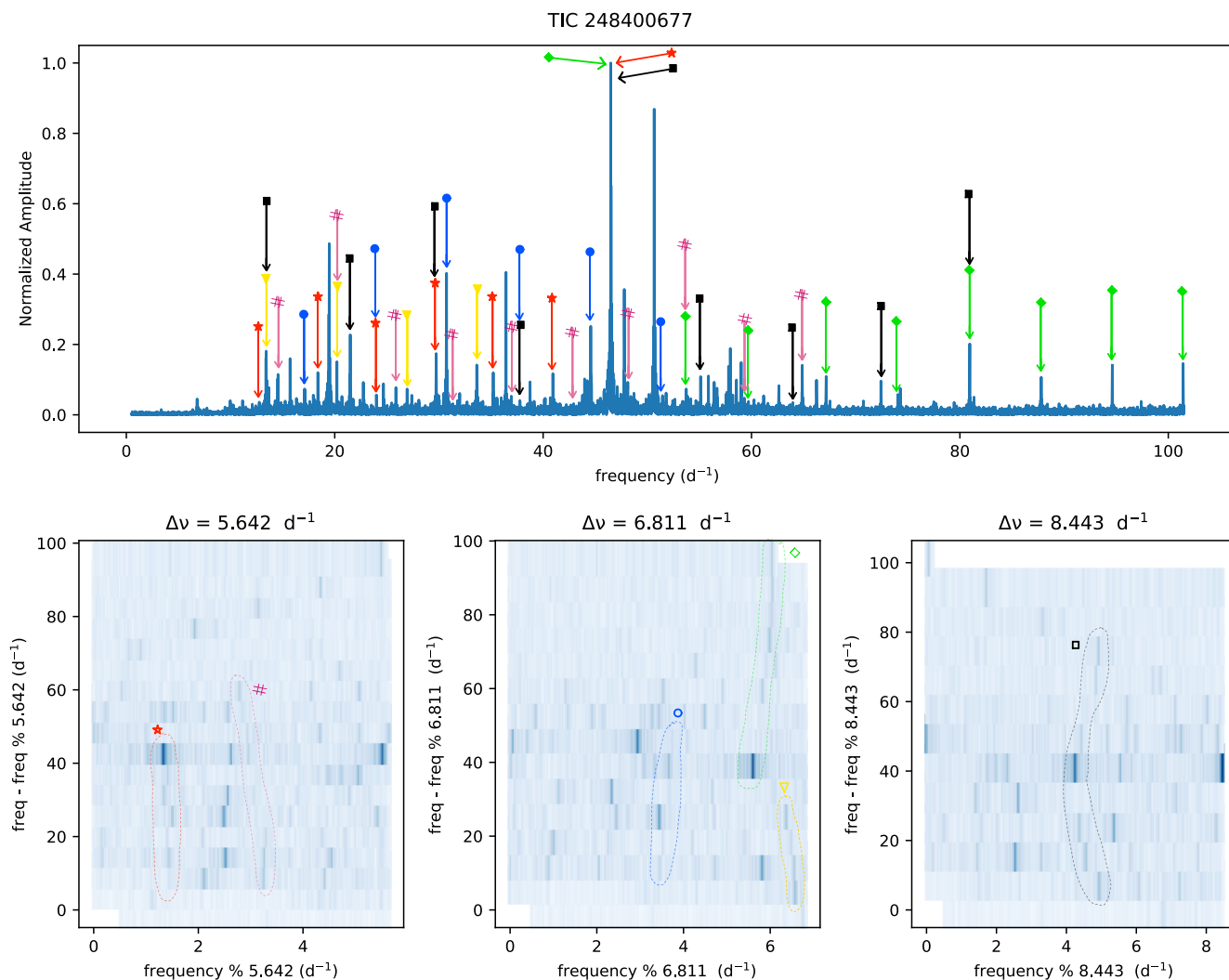


Figure 5. Normalized power spectrum and échelles at three values of large spacings for a δ Scuti. Each sequence in the échelle diagrams is marked using faint dashed lines of different colours. The modes corresponding to each sequence are identified in the power spectrum above. Some modes appear to be associated with two sequences (marked with two arrows) although the other unmarked peaks in the close vicinity might break this degeneracy. Almost every single significant mode is accounted for, approaching near-complete spectral quantization.

302 Paxton, B., Cantiello, M., Arras, P., et al. 2013, The
 303 Astrophysical Journal Supplement Series, 208, 4,
 304 doi: [10.1088/0067-0049/208/1/4](https://doi.org/10.1088/0067-0049/208/1/4)
 305 Paxton, B., Marchant, P., Schwab, J., et al. 2015, The
 306 Astrophysical Journal Supplement Series, 220, 15,
 307 doi: [10.1088/0067-0049/220/1/15](https://doi.org/10.1088/0067-0049/220/1/15)
 308 Paxton, B., Schwab, J., Bauer, E. B., et al. 2018, The
 309 Astrophysical Journal Supplement Series, 234, 34,
 310 doi: [10.3847/1538-4365/aaa5a8](https://doi.org/10.3847/1538-4365/aaa5a8)
 311 Paxton, B., Smolec, R., Schwab, J., et al. 2019, The
 312 Astrophysical Journal Supplement Series, 243, 10,
 313 doi: [10.3847/1538-4365/ab2241](https://doi.org/10.3847/1538-4365/ab2241)

314 Pérez Hernández, F., Claret, A., Hernández, M. M., &
 315 Michel, E. 1999, *A&A*, 346, 586
 316 Ramón-Ballesta, A., García Hernández, A., Suárez, J. C.,
 317 et al. 2021, *Monthly Notices of the Royal Astronomical*
 318 *Society*, 505, 6217–6224, doi: [10.1093/mnras/stab1719](https://doi.org/10.1093/mnras/stab1719)
 319 Reese, D., Lignières, F., & Rieutord, M. 2006, *A&A*, 455,
 320 621, doi: [10.1051/0004-6361:20065269](https://doi.org/10.1051/0004-6361:20065269)
 321 —. 2008, *A&A*, 481, 449–452,
 322 doi: [10.1051/0004-6361:20078075](https://doi.org/10.1051/0004-6361:20078075)
 323 Reese, D. R. 2022, *Frontiers in Astronomy and Space*
 324 *Sciences*, Volume 9 - 2022, doi: [10.3389/fspas.2022.934579](https://doi.org/10.3389/fspas.2022.934579)
 325 Reese, D. R., Lignières, F., Ballot, J., et al. 2017, *A&A*,
 326 601, A130, doi: [10.1051/0004-6361/201321264](https://doi.org/10.1051/0004-6361/201321264)

- 327 Reese, D. R., MacGregor, K. B., Jackson, S., Skumanich,
328 A., & Metcalfe, T. S. 2009, *A&A*, 506, 189,
329 doi: [10.1051/0004-6361/200811510](https://doi.org/10.1051/0004-6361/200811510)
- 330 Royer, F., Zorec, J., & Gómez, A. E. 2007, *A&A*, 463, 671,
331 doi: [10.1051/0004-6361:20065224](https://doi.org/10.1051/0004-6361:20065224)
- 332 Saio, H. 1981, *ApJ*, 244, 299, doi: [10.1086/158708](https://doi.org/10.1086/158708)
- 333 Sartoretti, P., Marchal, O., Babusiaux, C., et al. 2023,
334 *A&A*, 674, A6, doi: [10.1051/0004-6361/202243615](https://doi.org/10.1051/0004-6361/202243615)
- 335 Singh, K. H., Panda, S. K., Hanasoge, S. M., & Dhanpal, S.
336 2025, *The Astrophysical Journal*, 987, 175,
337 doi: [10.3847/1538-4357/add7df](https://doi.org/10.3847/1538-4357/add7df)
- 338 Zeipel, H. v. 1924, *Monthly Notices of the Royal*
339 *Astronomical Society*, 84, 665,
340 doi: [10.1093/mnras/84.9.665](https://doi.org/10.1093/mnras/84.9.665)